ALTERNATING CURRENT ELECTRO-OSMOTIC FLOW OF THE MAXWELL FLUIDS THROUGH A CIRCULAR MICRO-PIPE

L.-X. Sun **Y.-J. Jian** *

School of Mathematical Science
Inner Mongolia University
Hohhot, Inner Mongolia 010021, China

L. Chang

School of Mathematical Science
Inner Mongolia University
Hohhot, Inner Mongolia 010021, China

School of Mathematics and Statistics
Inner Mongolia Finance and Economics College
Hohhot, Inner Mongolia 010051, China

H.-Y. Zhang

College of Mathematical Science
Baotou teacher's college, Baotou
Inner Mongolia 014030, China

Q.-S. Liu

School of Mathematical Science
Inner Mongolia University
Hohhot, Inner Mongolia 010021, China

ABSTRACT

Analytical solutions are presented for time periodic EOF flow of linear viscoelastic fluids through a cylindrical micro-pipe. The linear viscoelastic fluids used here are described by the general Maxwell model. The solution involves analytically solving the linearized Poisson-Boltzmann equation, together with the Cauchy momentum equation and the general Maxwell constitutive equation considering the depletion effect produced by the interaction between macro-molecules of the Maxwell fluid and the channel surface. The overall flow is divided into depletion layer and bulk flow outside of depletion layer. The velocity expressions of these two layers were obtained, respectively. By numerical computations, the influences of the periodic EOF electric oscillating Reynolds number Re, Deborah number *De*, depletion layer thickness δ and the viscosity ratio γ of Maxwell to Newtonian fluids on velocity profile are presented. For a prescribed *De*, the increasing Re will cause large changes of the EOF velocity with decreasing velocity magnitude. For a given Re, large *De* gives large EOF velocity magnitude. Increasing γ will lead to larger velocity amplitude for a given lower Re. However, at higher Re, the velocity amplitude decreases with the viscosity ratio γ, especially within the depletion layer. In addition, large depletion layer thickness gives small EOF velocity magnitude for fixed Re and *De*. Finally, the influence of *De* on energy dissipation is studied. These results provide a detail insight of the flow characteristic of this flow configuration.

Keywords: Time periodic EOF, Generalized Maxwell fluids, Circular micro-pipe, Oscillating Reynolds number, Relaxation times, Viscosity ratio.

1. INTRODUCTION

Microfluidics devices have become important due to its potential applications as a tool for studying fundamental physical and biochemical processes and a platform for performing chemical and biological assays [1,2]. Electro-osmosis is often used as a means of transporting fluid in microchannels. An important feature of the electro-osmosis based microfluidic systems which gives them many advantages over other miniaturized mechanical devices is that they do not need any moving components.

In most of pratical applications, microfluidic devices mainly treat biofluids like polymer solutions, body fluids and blood. These complex fluids are made of long chain molecules and macromolecules. They behave obviously non-Newtonian characteristics, such as variable viscosity, memory effects, normal stress effect *etc*. These biofluids are often modeled by viscoelastic fluids such as Maxwell, power-law fluids, Phan-Thien-Tanner (PTT) and Jeffreys fluids *etc*. The open literature shows numerous studies involving power-law fluids of

* Corresponding author (jianyongjun@yahoo.com.cn)

DOI : 10.1017/jmech.2012.138
Copyright © 2013 The Society of Theoretical and Applied Mechanics, R.O.C.
https://doi.org/10.1017/jmech.2012.138 Published online by Cambridge University Press

electroosmotic flow (EOF) in microchannels [3-8]. They computed the velocity profiles which depend on the power law index n. The extension to viscoelastic fluids was done by Park and Lee [9,10], Jian and Liu [11,12]. Afonso *et al*. [13] derived an analytical solution for the combined electroosmosis-Poiseuille flow of PTT model [14] in a parallel plane channel. Dhinakaran *et al*. [15] extended the work of Alonso *et al*. [13] by considering the full Gordon-schowalter convective derivative in the PTT model. All the foregoing investigations assume that fluid properties are uniform in the whole domain. Nevertheless, such as a situation is hardly found in experiments, as long as polymer solutions are considered. In fact, due to the unavoidable interaction between macro-molecules and the channel surface, polymer depletion and adsorption phenomena will be produced [16]. Sousa and Afonsa [17] investigated the effects of the depletion layer on electroosmotic Poiseuille flows of PTT fluids. Liu *et al*. [18] studied AC EOF of the Jeffreys fluids through a slit microchannel by considering the effects of the depletion layer.

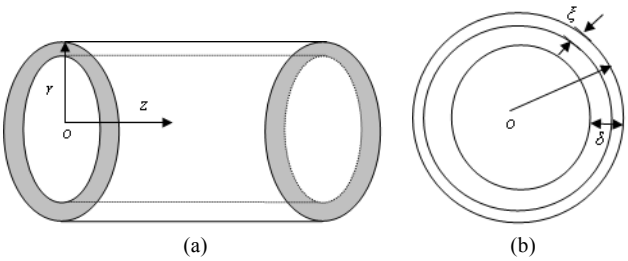
Maxwell fluid model is a non-Newtonian fluid model. Very recently, Maxwell fluid model was used for modeling blood flow through a tapered artery with a stenosis [19]. The blood and other biofluids are often analyzed in a blood-based microfluidic transport system by means of electrokinetic mechanisms. Therefore, we select Maxwell fluid model as a constitutive relation to describe AC EOF in a circular microchannel in present work. The purpose of this paper is extending our work [11] between two micro-parallel plates to a circular microtube taking the depletion layer effect into account.

2. PROBLEM FORMULATION

2.1 Cauchy Momentum Equation and Constitutive Relation

The unsteady EOF of the incompressible Maxwell fluids through a negatively charged cylindrical micropipe, whose radius is R, is sketched in Fig. 1. The length of the pipe is L, assumed to be much larger than the radius, *i.e.* $L>>R$. A cylindrical coordinate system is introduced, where r- and z-axis are radical and the flow of the fluids direction, respectively. The depletion layer is produced by interaction between macromolecules and the channel surface. The concentration of no adsorbing particles decreases steeply near smooth surfaces, leaving a depleted layer has a thickness δ^*, which is larger than the thickness ξ of the Electric double layer (EDL) and smaller than radius R of the micropipe [20]. The viscosity of this layer is much lower than that of the bulk. Thus, the depletion layer can be modeled by Newtonian fluid and the bulk fluids are modeled by viscoelastic Maxwell fluid model (see Fig. 1).

Provided that the pressure gradient along z direction is ignored, the one-dimensional Cauchy momentum equation can be expressed as



(a) (b)

Fig. 1. (a) Sketch of time periodic EOF flow of the generalized Maxwell fluids through a circular microchannel along z direction. (b) Cross section of the microtube

$$\rho\frac{\partial u(r,\ t)}{\partial t}=-\frac{1}{r}\frac{\partial}{\partial r}(r\tau_{rz})+\rho_e(r)E(t) \tag{1}$$

where $u(r,\ t)$ is the axial velocity, which is along positive z direction, ρ is the fluid density, t is time, τ_{rz} is the stress tensor, $\rho_e(r)$ is volume charge density, and $E(t)$ is AC electric field. In the depletion layer (layer I), the stress tensor can be described by Newtonian fluid with viscosity μ

$$\tau_{rz}^{I}=-\mu\frac{\partial u^{I}(r,\ t)}{\partial r} \tag{2}$$

where $u^I(r,\ t)$ and τ^I_{rz} mean the velocity and stress tensors in layer I, respectively. Whereas elsewhere the fluid, *i.e.*, polymeric liquid (layer II), is described by the Maxwell model, and its constitutive equation of differential form satisfies

$$\tau_{rz}^{II}+\lambda\frac{\partial\tau_{rz}^{II}}{\partial t}=-\eta_0\frac{\partial u^{II}(r,\ t)}{\partial r} \tag{3}$$

where $u^{II}(r,\ t)$ and τ^{II}_{rz} mean the velocity and stress tensors in layer II, λ is the relaxation time and η_0 is the zero shear rate viscosity. For steady motions Eq. (3) simplifies to the Newtonian fluid with viscosity η_0. For sudden changes in stress, the time derivative term dominates the left side of the Eq. (3), and then integration with respect to time gives the Hookean elastic solid. Maxwell fluid is the simplest expression for the shear stress for a fluid that is both viscous and elastic.

Recognizing Eq. (3) is a first-order, linear equation for stress as a function of t, which can be integrated at once to give

$$\tau_{rz}^{II}=-\int_{-\infty}^{t}\left\{\frac{\eta_0}{\lambda}\exp\left[-\frac{(t-t')}{\lambda}\right]\frac{\partial u^{II}(r,\ t')}{\partial r}\right\}dt' \tag{4}$$

At the above equation, the stress at the present time t depends on the rate of strain at all past times t', with a weighting factor that decays exponentially as one goes backwards in time. The fluid remembers very well what it has experienced in the very recent past but has only a hazy recollection of events in the distant past. That is to say, the stress at time t depends on the "history" of the rate of strain for all past times from $-\infty$ to t. This phenomenon is called "fading memory" effect [12].

https://doi.org/10.1017/jmech.2012.138 Published online by Cambridge University Press

We suppose AC electric field and velocity of periodic EOF can be written in complex forms as

$$u^I(r,\ t) = \Re\left\{u_0^I(r)e^{i\omega t}\right\}\ , \tag{5a}$$

$$u^{II}(r,\ t) = \Re\left\{u_0^{II}(r)e^{i\omega t}\right\}\ , \tag{5b}$$

$$E(t) = \Re\{E_0\ e^{i\omega t}\} \tag{5c}$$

where the $\Re\ \{\}$ denotes the real part of the function, ω is imposed AC electric field oscillating angular frequency, E_0, $u_0^I(r)$, and $u_0^{II}(r)$ are amplitudes of AC electric field, layer I and II velocities, respectively. Substituting Eq. (5b) into Eq. (4), we get

$$\tau_{rz}^{II} = \Re\left\{-\frac{\eta_0}{\lambda}\frac{du_0^{II}(r)}{dr}\int_{-\infty}^{t}\exp\left[-\frac{(t-t')}{\lambda}\right]\ \exp(i\omega t')\ dt'\right\} \tag{6}$$

After computing right hand side of the integral of Eq. (6), we have

$$\tau_{rz}^{II} = -\eta_0\ \Re\left\{\frac{du_0^{II}(r)}{dr}\frac{1}{1+i\lambda\omega}e^{i\omega t}\right\} \tag{7}$$

For layer I, substituting Eqs. (2) and (5a, 5c) into Eq. (1), removing the real-operator sign and multiplier $e^{i\omega t}$ from both sides, we have

$$r^2\frac{d^2u_0^I(r)}{dr^2} + r\frac{du_0^I(r)}{dr} - \frac{\rho_1}{\mu}i\omega r^2u_0^I(r) = -\frac{\rho_e}{\mu}r^2E_0 \tag{8}$$

where ρ_1 is the fluid density of Newtonian fluids. Similarly, for layer II, substitute Eqs. (5b, 5c) and (7) into Eq. (1), we get

$$r^2\frac{d^2u_0^{II}(r)}{dr^2} + r\frac{du_0^{II}(r)}{dr} - \frac{\rho_2}{\eta_0}i\omega(1+i\lambda\omega)r^2u_0^{II}(r) = -\frac{\rho_e}{\eta_0}(1+i\lambda\omega)r^2E_0 \tag{9}$$

where ρ_2 is the fluid density of Maxwell fluid.

2.2 Boundary Conditions

For layer I, no-slip condition at the wall should be satisfied

$$u_0^I(r)\big|_{r=R} = 0 \tag{10}$$

At the interface between the depletion layer and the bulk of the fluid, both fluids move at the same velocity

$$u_0^I(r)\,|_{r=R-\delta^*} = u_0^{II}(r)\,|_{r=R-\delta^*} \tag{11}$$

where δ^* is the thickness of depletion layer.

For layer II, besides velocity continue condition of Eq. (11), the flow symmetry condition of centre-plane should be satisfied

$$\frac{du_0^{II}(r)}{dr}\,|_{r=0} = 0 \tag{12}$$

In addition, shear stress at the interface between layer I and layer II should be equal

$$\tau_{rz}^I\,|_{r=R-\delta^*} = \tau_{rz}^{II}\,|_{r=R-\delta^*} \tag{13}$$

2.3 Charge Density Distributions

For a symmetric electrolyte solution and thin EDL, the net charge density $\rho_e(r)$ within the EDL is given by the following Possion-Boltzmann (PB) equation:

$$\nabla^2\psi = -\frac{\rho_e(r)}{\varepsilon}\ ,$$

where

$$\rho_e(r) = -2n_0\ z_v\ e\sinh\left(\frac{z_v\ e\psi}{k_b\ T}\right) \tag{14a, 14b}$$

where ε is the dielectric constant of the electrolyte liquid, ψ denotes the electrical potential of the EDL, n_0 is the ion density of bulk liquid, z_v is the valence, e is the electron charge, k_b is the Boltzmann constant, and T is absolute temperature. For small values of electrical potential ψ within the EDL, the Debye-Hückel linearization approximation can be applied, which means physically that the electrical potential is small compared with the thermal energy of the charged species. Combining Eqs. (14a) and (14b), we have

$$\nabla^2\psi = k^2\psi \tag{15}$$

where $k = (2n_0\ z_v^2e^2/\varepsilon k_b\ T)^{1/2}$ is the Debye-Hückel parameter and $1/k$ denotes the thickness of the EDL. The boundary conditions of Eq. (15) are

$$\psi\,|_{r=R} = \psi_s\ ,\quad \frac{d\psi}{dr}\,|_{r=0} = 0 \tag{16a, 16b}$$

where ψ_s is the wall zeta potential of the microtube. The solution of electrical potential can be obtained by Eqs. (15) and (16). Furthermore, the charge density can be expressed as

$$\rho_e(r) = -\varepsilon k^2\psi_s\frac{I_0(kr)}{I_0(kR)} \tag{17}$$

2.4 Analytical Solution of EOF Velocity

For simplicity, the following dimensionless groups are introduced:

$$\bar{r} = \frac{r}{R}\ ,\ K = kR\ ,\ \bar{u}_0^I(\bar{r}) = \frac{u_0^I(r)}{U_{eo}}\ ,\ \bar{u}_0^{II}(\bar{r}) = \frac{u_0^{II}(r)}{U_{eo}}\ ,$$
$$U_{eo} = -\frac{\varepsilon\psi_s\ E_0}{\mu}\ ,\ De = \lambda\omega$$
$$\mathrm{Re} = \frac{R^2\rho_1\ \omega}{\mu}\ ,\ \gamma = \frac{\eta_0}{\mu}\ ,\ \delta = \frac{\delta^*}{R}\ ,\ \rho = \frac{\rho_2}{\rho_1} \tag{18}$$

https://doi.org/10.1017/jmech.2012.138 Published online by Cambridge University Press

where K is called the non-dimensional electrokinetic width denoting the ratio of microtube radius R to Debye length, U_{eo} denotes steady Helmholtz-Smoluchowski EOF velocity of Newtonian fluid between slit microchannel or in a cylindrical capillary, De number is defined as the ratio of relaxation time λ of the fluid to oscillating time $1/\omega$ of electric field, Re means electric oscillating Reynolds number [21], γ is viscosity ratio of Maxwell fluid to Newtonian fluid and δ is normalized depletion layer thickness.

For layer I, using Eqs. (17) and (18), the electroosmosis Eq. (8) is normalized as

$$\frac{d^2\bar{u}_0^I(\bar{r})}{d\bar{r}^2}+\frac{1}{\bar{r}}\frac{d\bar{u}_0^I(\bar{r})}{d\bar{r}}-i\,\mathrm{Re}\,\bar{u}_0^I(\bar{r})=-K^2\frac{I_0(Kr)}{I_0(K)} \tag{19}$$

Equation (19) is a second-order inhomogeneous ordinary differential equation for the complex function $\bar{u}_0^I(\bar{r})$. Its general solution can be written as

$$\bar{u}_0^I(\bar{r})=C_1I_0(\sqrt{i\,\mathrm{Re}}\bar{r})+C_2K_0(\sqrt{i\,\mathrm{Re}}\bar{r})+AI_0(K\bar{r}) \tag{20}$$

Substituting Eq. (20) into Eq. (19), constant A can be determined as

$$A=\frac{K^2}{i\,\mathrm{Re}-K^2}\frac{1}{I_0(K)} \tag{21}$$

Thus Eq. (20) can be written as

$$\bar{u}_0^I(\bar{r})=C_1\,I_0(\sqrt{i\,\mathrm{Re}}\bar{r})+C_2\,K_0(\sqrt{i\,\mathrm{Re}}\bar{r})+\frac{K^2}{i\,\mathrm{Re}-K^2}\frac{1}{I_0(K)}I_0(K\bar{r}) \tag{22}$$

The coefficients of C_1 and C_2 will be determined by boundary conditions later.

For layer II, using Eqs. (17) and (18), The Cauchy momentum equation (9) is normalized as

$$\frac{d^2\bar{u}_0^{II}(\bar{r})}{d\bar{r}^2}+\frac{1}{\bar{r}}\frac{d\bar{u}_0^{II}(\bar{r})}{d\bar{r}}-i(1+iDe)\,\mathrm{Re}\,\rho\frac{1}{\gamma}\bar{u}_0^{II}(\bar{r})=-(1+iDe)\frac{1}{\gamma}K^2\frac{1}{I_0(K)}I_0(K\bar{r}) \tag{23}$$

Using Eq. (18), boundary conditions (10-13) are normalized as

$$\bar{u}_0^I(\bar{r})\,|_{\bar{r}=1}=0 \tag{24a}$$

$$\bar{u}_0^I(\bar{r})\,|_{\bar{r}=1-\delta}=\bar{u}_0^{II}(\bar{r})\,|_{\bar{r}=1-\delta} \tag{24b}$$

$$\frac{d\bar{u}_0^{II}(\bar{r})}{d\bar{r}}\,|_{\bar{r}=0}=0 \tag{24c}$$

$$\frac{d\bar{u}_0^I(\bar{r})}{d\bar{r}}\,|_{\bar{r}=1-\delta}=\frac{\gamma}{1+iDe}\frac{d\bar{u}_0^{II}(\bar{r})}{d\bar{r}}\,|_{\bar{r}=1-\delta} \tag{24d}$$

Similarly, the general solution of Eq. (23) can be written as

$$\bar{u}_0^{II}(\bar{r})=C_3\,I_0\left(\sqrt{i\,\mathrm{Re}\,\rho(1+iDe)\frac{1}{\gamma}}\bar{r}\right)+C_4K_0\left(\sqrt{i\,\mathrm{Re}\,\rho(1+iDe)\frac{1}{\gamma}}\bar{r}\right)-\frac{(1+iDe)\,K^2}{I_0(K)}\frac{1}{K^2\gamma-i\,\mathrm{Re}\,\rho(1+iDe)}I_0(K\bar{r}) \tag{25}$$

Finally, from velocity expressions (22) and (25) and boundary conditions (24), four constants C_1, C_2, C_3 and C_4 can be determined. Their detail expressions can be found in appendix A.

2.5 Energy Dissipation in Each Constitutive Component

For the linear viscoelastic Maxwell fluid, it is important in characterizing the behavior of a material. If the complex modulus G^* and complex viscosity η^* are defined by $\tau_{rz}=-G^*\gamma_{rz}$ and $\tau_{rz}=-\eta^*\dot{\gamma}_{rz}$, (where γ_{rz} and $\dot{\gamma}_{rz}$ are shear strain and shear rate, respectively) and we take $G^*=G'+iG''$, $\eta^*=\eta'-i\eta''$, then for a perfectly elastic solid G'' is equal to the constant shear modulus G, and G' is zero; whereas for a Newtonian fluids, η' is equal to viscosity μ, and η'' is zero. For this reason $G'(=\eta''\omega)$ gives information about the elastic character of the fluid or the energy storage that takes place during the deformation. On the other hand, $G''(=\eta'\omega)$ tells about the viscous character of the fluid, or the energy dissipation that occurs in flow. The dimensional energy dissipated per unit volume within one oscillating period can be expressed as

$$W=\int_0^{2\pi/\omega}\tau_{rz}^I\,\dot{\gamma}_{rz}^I\,dt+\int_0^{2\pi/\omega}\tau_{rz}^{II}\,\dot{\gamma}_{rz}^{II}\,dt \tag{26}$$

where $\dot{\gamma}_{rz}^I$ and $\dot{\gamma}_{rz}^{II}$ are shear rates for Newtonian and Maxwell fluids in depletion layer and our of depletion layer, respectively. Substituting shear stress and velocity gradient from Eqs. (2), (5), (7), (22) and (25) to Eq. (26), the dissipated energy is

$$\begin{aligned}W_d&=\int_0^{2\pi/\omega}\mu\left(\frac{U_{eo}}{R}\right)^2\left(\frac{d\bar{u}_0^I(\bar{r})}{d\bar{r}}\right)^2\cos^2(\omega t)\,dt\\&+\int_0^{2\pi/\omega}\frac{\eta_0}{1+De^2}\left(\frac{U_{eo}}{R}\right)^2\left(\frac{d\bar{u}_0^{II}(\bar{r})}{d\bar{r}}\right)^2\left[\cos^2(\omega t)+De\cos(\omega t)\sin(\omega t)\right]dt\\&=\frac{\pi}{\omega}\left(\frac{U_{eo}}{R}\right)^2\left[\mu\left(\frac{d\bar{u}_0^I(\bar{r})}{d\bar{r}}\right)^2+\frac{\eta_0}{1+De^2}\left(\frac{d\bar{u}_0^{II}(\bar{r})}{d\bar{r}}\right)^2\right]\end{aligned} \tag{27}$$

So the normalized dissipated energy can be written as

$$\bar{W}_d=W_d/\frac{\pi\mu}{\omega}\left(\frac{U_{eo}}{R}\right)^2=\left(\frac{d\bar{u}_0^I(\bar{r})}{d\bar{r}}\right)^2+\frac{\gamma}{1+De^2}\left(\frac{d\bar{u}_0^{II}(\bar{r})}{d\bar{r}}\right)^2 \tag{28}$$

https://doi.org/10.1017/jmech.2012.138 Published online by Cambridge University Press

where

$$\frac{d\bar{u}_0^I(\bar{r})}{d\bar{r}} = \sqrt{i\,\mathrm{Re}}\left[C_1 I_1(\sqrt{i\,\mathrm{Re}}\bar{r}) - C_2 K_1(\sqrt{i\,\mathrm{Re}}\bar{r})\right] + \frac{K^3}{i\,\mathrm{Re} - K^2}\frac{1}{I_0(K)} I_1(K\bar{r})$$

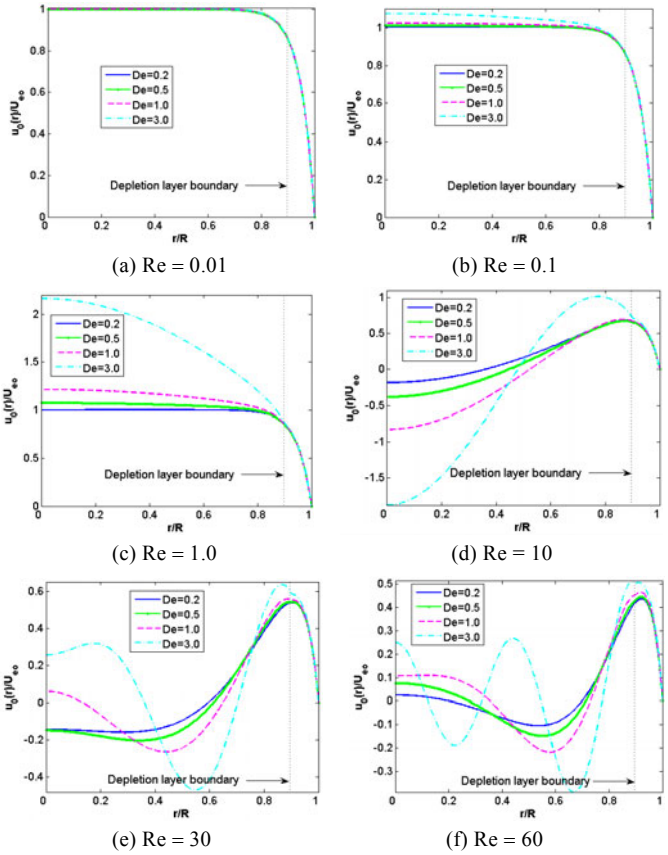
$$\frac{d\bar{u}_0^{II}(\bar{r})}{d\bar{r}} = C_3\sqrt{i\,\mathrm{Re}\frac{\rho}{\gamma}(1+iDe)} \times I_1\left(\sqrt{i\,\mathrm{Re}\frac{\rho}{\gamma}(1+iDe)}\bar{r}\right) - \frac{(1+iDe)\,K^3}{I_0(K)}\frac{1}{K^2\gamma - i\,\mathrm{Re}\,\rho(1+iDe)} I_1(K\bar{r}) \quad (29a,29b)$$

3. RESULTS AND DISCUSSIONS

In the section 2, analytical solutions were derived for the periodic EOF flow of Maxwell fluids through a cylindrical micro-pipe. They depend mainly on the electrokinetic width $K=Rk$, viscosity ratio γ, the periodical EOF electric oscillating Reynolds number $\mathrm{Re} = \rho_1\omega R^2/\mu$, depletion layer thickness δ and the Deborah number De. In practical engineering problems, the parametric regions of Re and Deborah number De are wide due to wide parameter values of ω, μ, λ [22]. In the following calculations, the influence of the above mentioned parameters on velocity amplitudes are investigated.

Some parametric ranges must be determined before we carry out numerical computations. Moreover, the relaxation time should be smaller than the oscillation period (observation time), *i.e.* $\lambda < 2\pi/\omega$ or $De < 2\pi$ must be satisfied. In our calculations, typical parameters can be taken as follows: $\rho_1 = 1.06 \times 10^3$ kg.m^{-3}, $\mu = 10^{-3}$kg.m^{-1}s^{-1}, $R = 100\mu$m, $\mu \le \eta_0 \le 3\mu$. The parametric regions of the external electric field frequency ω changes from 0 to 1.6kHz, corresponding to angle frequency changes from 0 to 10^4s^{-1}. Thus, oscillating Reynolds number Re can be evaluated changed from 0 to 100 [22,23]. From Ref. [20], the thickness of the depletion layer δ^* is taken as $\delta^*/R = 0.1$ in the following Fig. 2 to Fig. 4. Additionally, the real part of $u_0(r)/U_{eo}$ in all figures was taken.

When $K = 20$, Fig. 2 shows the effects of Deborah number De (0.2, 0.5, 1.0, and 3.0) on the normalized EOF velocity amplitudes of Maxwell fluid across half channel width for different Re (0.01, 0.1, 1.0, 10, 30, and 60). From Fig. 2 (a), as is expected, when $\gamma = 1$ and $\rho = 1$, a classical plug-liked velocity profile is reduced for small Re. This case indeed is similar to single layer Newtonian fluid. For a given De, the increasing Re will cause large changes of velocity profile of EOF. Meanwhile the magnitude of the velocity amplitude becomes small. The main reason is that there is no sufficient time for the flow to diffuse far into the mid-plane of the wall, and the EOF velocity variations are restricted only within the EDL. In addition, for the general Maxwell fluids, if the De number is large, polymer molecules that are distorted by the flow will not have time to relax during the time scale of the

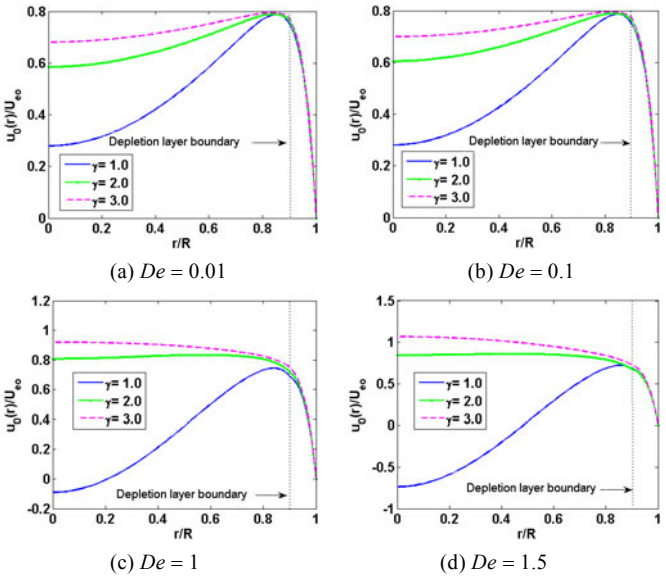


(a) Re = 0.01 (b) Re = 0.1

(c) Re = 1.0 (d) Re = 10

(e) Re = 30 (f) Re = 60

Fig. 2 Normalized EOF velocity of generalized Maxwell fluid across a cylinder pipe for Deborah number De (0.2, 0.5, 1.0, and 3.0) for different oscillating Reynolds number Re (0.01, 0.1, 1.0, 10, 30, and 60), (K = 20, γ = 1, ρ = 1, δ = 0.1)

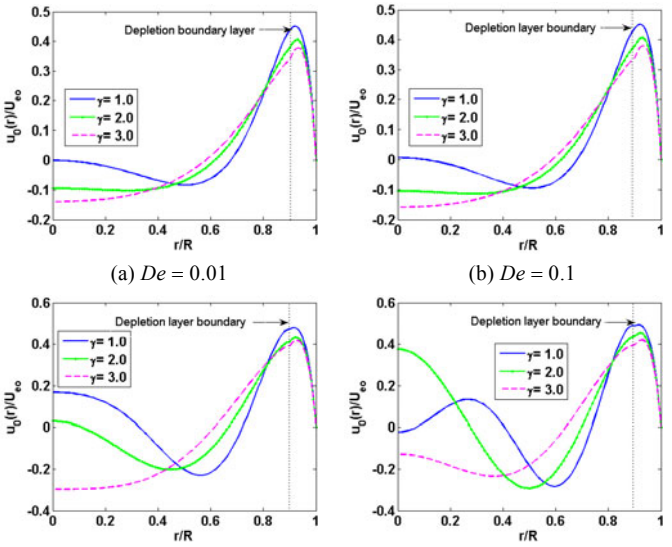


(a) De = 0.01 (b) De = 0.1

(c) De = 1 (d) De = 1.5

Fig. 3 Effects of the viscosity ratio γ of Maxwell fluid to Newtonian fluid on the normalized EOF velocity amplitudes of Maxwell fluid for different Deborah number De (K = 20, Re = 5, ρ = 1.1, δ = 0.1)

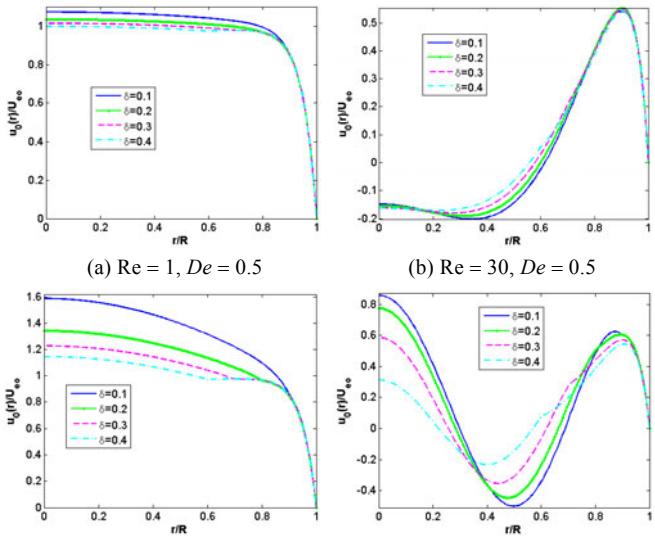
https://doi.org/10.1017/jmech.2012.138 Published online by Cambridge University Press



(a) De = 0.01 (b) De = 0.1

(c) De = 1 (d) De = 1.5

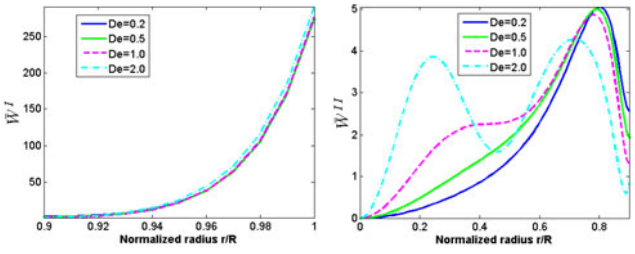
Fig. 4 Effects of the viscosity ratio γ of Maxwell fluid to Newtonian fluid on the normalized EOF velocity amplitudes of Maxwell fluid for different Deborah number De (K = 20, Re = 50, ρ = 1.1, δ = 0.1)



(a) Re = 1, De = 0.5 (b) Re = 30, De = 0.5

(c) Re = 1, De = 2 (d) Re = 30, De = 2

Fig. 5 Effects of the depletion layer thickness on the normalized EOF velocity amplitudes for different Re and De (K = 20, γ = 1, ρ = 1.)



(a) Dissipated energy for layer I (b) Dissipated energy for layer II

Fig. 6 Normalized dissipated energy per unit volume with different Deborah number De (0.2, 0.5, 1.0, and 2.0), (K = 20, Re = 30, γ = 1, ρ = 1, δ = 0.1)

oscillation. Further increasing De will lead to the flow process happens so fast that the polymer molecules have no time to change configuration, and the fluid behaves more and more as a Hookean elastic solid. For a given Re, large De gives large EOF velocity magnitude.

When K = 20, Figs. 3 and 4 show the effects of the viscosity ratio γ of Maxwell to Newtonian fluids on the velocity amplitudes for different De (0.01, 0.1, 1.0, 1.5) when Re = 5 and Re = 50 respectively. From Fig. 3, we find that the increasing γ will lead to larger velocity amplitude for a given lower Re. With the increase of De, the amplitude of EOF velocity becomes larger no matter whether γ is large or not. The reason is that in case of small Re (low oscillating frequency or high viscosity of Newtonian fluid), the De number becomes small and the whole flow behaves more like viscous Newtonian fluid. With the increase of γ, the shear stress between the two layers becomes larger, which leads to the larger normalized EOF velocity.

However, at higher Re, it can be found in Fig. 4 that the velocity amplitude decreases with the viscosity ratio γ no matter whether De is large or not, especially within the depletion layer. The main reason is that in case of larger Re (high oscillating frequency or low viscosity of Newtonian fluid), the De number becomes large and the whole flow behaves more like Hookean elastic solid. In this situation, increasing γ means that the viscosity decreases in Newtonian fluid due to unchangeable viscosity of the viscoelastic fluid. Thus the shear stress between the two layers becomes smaller, which leads to the smaller normalized EOF velocity.

Figure 5 illustrated the influences of the depletion layer thickness δ on the normalized EOF velocity amplitudes for different Re and De. From Fig. 5, we found large depletion layer thickness gives small EOF velocity magnitude for fixed Re and De. Physically, thick depletion layer means larger spectrum occupied by Newtonian fluid in flow field, which produces smaller velocity amplitude [11].

Normalized dissipated energy per unit volume for generalized Maxwell fluid with different Deborah number De (0.2, 0.5, 1.0, and 2.0) is shown in Fig. 6. It can be seen from Fig. 6 that the influence of De on energy dissipation is very small in depletion layer. Physically, the reason is that energy dissipation is caused by Newtonian fluids and mainly focused on depletion layer. However, within the outside of depletion layer, larger De number leads to larger energy dissipation for Maxwell fluids. In addition, energy dissipation in layer I is greatly larger than that in layer II no matter whether De number is large or not.

4. CONCLUSIONS

An analytical solution of the time periodic EOF flow of Maxwell fluids through a microtube is presented in this work. The solution involves solving the PB equations, together with the Cauchy momentum equation

https://doi.org/10.1017/jmech.2012.138 Published online by Cambridge University Press

and the Maxwell constitutive equation taking the depletion effect produced by interaction between macromolecules of the Maxwell fluid and the channel surface into account. The overall flow is divided into depletion layer and bulk flow outside of depletion layer. The velocity expressions of these two layers were obtained, respectively. We found the velocity amplitude of Maxwell fluid depends greatly on the viscosity ratio γ, oscillating Reynolds number Re, Deborah number *De* and the thickness of depletion layer δ.

By numerical computations, we can draw the following conclusions:

1. When $\gamma = 1$ and $\rho = 1$, a classical single layer plug-liked velocity profile of Newtonian fluid is reduced for small Re. For a prescribed *De*, the increasing Re will cause large changes of the EOF velocity with decreasing velocity magnitude. For a given Re, large *De* gives large EOF velocity magnitude.
2. Increasing γ will lead to larger velocity amplitude for a given lower Re. With the increase of *De*, the amplitude of EOF velocity becomes larger no matter whether γ is large or not. However, at higher Re, the velocity amplitude decreases with the viscosity ratio γ no matter whether *De* is large or not, especially within the depletion layer.
3. Large depletion layer thickness gives small EOF velocity magnitude for fixed Re and *De*.
4. The influence of *De* on energy dissipation is very small in depletion layer. However, within the outside of depletion layer, larger energy dissipation will be produced for larger *De* number. In addition, energy dissipation in layer I is greatly larger than that in layer II no matter whether *De* number is large or not.

ACKNOWLEDGEMENTS

The work was supported by Ph.D. Programs Foundation of Ministry of Education of China (No. 20111501120001), Opening fund of State Key Laboratory of Nonlinear Mechanics, the National Natural Science Foundation of China (No. 11062005, 11202092), the Natural Science Foundation of Inner Mongolia (Grant No. 2010BS0107, 2012MS0107), the research start up fund for excellent talents at Inner Mongolia University (Grant No. Z20080211) and the support of Natural Science Key Fund of Inner Mongolia (Grant No. 2009ZD01).

APPENDIX

$$
\begin{aligned}
C_1 = &\left\{\frac{K^2}{i\,\mathrm{Re}-K^2}\frac{1}{I_0(K)}K_0(\sqrt{i\,\mathrm{Re}})\times\left[KI_1\left(K(1-\delta)\right)I_0\left(\sqrt{i\,\mathrm{Re}\rho(1+iDe)\frac{1}{\gamma}}(1-\delta)\right)\right.\right.\\
&\left.-\frac{\gamma}{1+iDe}\sqrt{i\,\mathrm{Re}\rho(1+iDe)\frac{1}{\gamma}}I_0\left(K(1-\delta)\right)I_1\left(\sqrt{i\,\mathrm{Re}\rho(1+iDe)\frac{1}{\gamma}}(1-\delta)\right)\right]\\
&+\frac{K^2}{i\,\mathrm{Re}-K^2}\left[\frac{\gamma}{1+iDe}\sqrt{i\,\mathrm{Re}\rho(1+iDe)\frac{1}{\gamma}}I_1\left(\sqrt{i\,\mathrm{Re}\rho(1+iDe)\frac{1}{\gamma}}(1-\delta)\right)\right.\\
&\left.\times K_0\left(\sqrt{i\,\mathrm{Re}}(1-\delta)+\sqrt{i\,\mathrm{Re}}I_0\left(\sqrt{i\,\mathrm{Re}\rho(1+iDe)\frac{1}{\gamma}}(1-\delta)\right)K_1(\sqrt{i\,\mathrm{Re}}(1-\delta)\right)\right]\\
&+\frac{\gamma K^2}{I_0(K)}\frac{1}{i\,\mathrm{Re}(1+iDe)\,\rho-K^2\gamma}K_0(\sqrt{i\,\mathrm{Re}})\\
&\times\left[\sqrt{i\,\mathrm{Re}\rho(1+iDe)\frac{1}{\gamma}}I_1\left(\sqrt{i\,\mathrm{Re}\rho(1+iDe)\frac{1}{\gamma}}(1-\delta)\right)I_0\left(K(1-\delta)\right)\right.\\
&\left.\left.-KI_0\left(\sqrt{i\,\mathrm{Re}\rho(1+iDe)\frac{1}{\gamma}}(1-\delta)\right)I_1\left(K(1-\delta)\right)\right]\right\}/\\
&\left\{\frac{\gamma}{1+iDe}\sqrt{i\,\mathrm{Re}\rho(1+iDe)\frac{1}{\gamma}}I_1\left(\sqrt{i\,\mathrm{Re}\rho(1+iDe)\frac{1}{\gamma}}(1-\delta)\right)\right.\\
&\times\left[I_0\left(\sqrt{i\,\mathrm{Re}}(1-\delta)\right)K_0(\sqrt{i\,\mathrm{Re}})-I_0(\sqrt{i\,\mathrm{Re}})K_0\left(\sqrt{i\,\mathrm{Re}}(1-\delta)\right)\right]\\
&-\sqrt{i\,\mathrm{Re}}I_0\left(\sqrt{i\,\mathrm{Re}\rho(1+iDe)\frac{1}{\gamma}}(1-\delta)\right)\\
&\left.\times\left[I_1\left(\sqrt{i\,\mathrm{Re}}(1-\delta)\right)K_0(\sqrt{i\,\mathrm{Re}})+I_0(\sqrt{i\,\mathrm{Re}})K_1\left(\sqrt{i\,\mathrm{Re}}(1-\delta)\right)\right]\right\}
\end{aligned}
\tag{A1}
$$

https://doi.org/10.1017/jmech.2012.138 Published online by Cambridge University Press

$$C_2 = \frac{-C_1 I_0(\sqrt{i\,\mathrm{Re}}) - \dfrac{K^2}{i\,\mathrm{Re} - K^2}}{K_0(\sqrt{i\,\mathrm{Re}})} \tag{A2}$$

$$C_3 = \left\{ C_1 I_0\left(\sqrt{i\,\mathrm{Re}}(1-\delta)\right) + C_2 K_0\left(\sqrt{i\,\mathrm{Re}}(1-\delta)\right) + \frac{K^2}{i\,\mathrm{Re} - K^2}\frac{1}{I_0(K)} I_0\left(K(1-\delta)\right) - \frac{(1+iDe)K^2}{I_0(K)}\frac{I_0\left(K(1-\delta)\right)}{i\,\mathrm{Re}(1+iDe)\,\rho - K^2\gamma} \right\} / I_0\left(\sqrt{i\,\mathrm{Re}\rho(1+iDe)\frac{1}{\gamma}}(1-\delta)\right) \tag{A3}$$

$$C_4 = 0 \tag{A4}$$

REFERENCES

1. Stone, H. A., Stroock, A. D. and Ajdari, A., "Engineering Flows in Small Devices: Microfluidics Toward a Lab-On-A-Chip," *Annual Review of Fluid Mechanics*, **36**, pp. 381–411 (2004).
2. Bayraktar, T. and Pidugu, S. B., "Characterization of Liquid Flows in Microfluidic Systems," *International Journal of Heat and Mass Transfer*, **49**, pp. 815–824 (2006).
3. Das, S. and Chakraborty, S., "Analytical Solutions for Velocity, Temperature and Concentration Distribution in Electroosmotic Micro-Channel Flows in a Non-Newtonian Bio-Fluid," *Analytical Chimica Acta*, **559**, pp. 15–24 (2006).
4. Chakraborty, S., "Electroosmotically Driven Capillary Transport of Typical Non-Newtonian Biofluids in Rectangular Microchannels," *Analytical Chimica Acta*, **605**, pp. 175–184 (2007).
5. Zhao, C., Zholkovskij, E., Masliyah, J. H. and Yang, C., "Analysis of Electroosmotic Flow of Power-Law Fluids in a Slit Microchannel," *Journal of Colloid and Interface Science*, **326**, pp. 503–510 (2008).
6. Vasu, N. and De, S., "Electroosmotic Flow of Power-Law Fluids at High Zeta Potentials," *Colloids and Surfaces A: Physicochemical and Engineering Aspects*, **368**, pp. 44–52 (2010)
7. Zhao, C. and Yang, C., "Nonlinear Smoluchowski velocity for Electroosmosis of Power-Law Fluids Over a Surface with Arbitrary Zeta Potentials," *Electrophoresis*, **31**, pp. 973–979 (2010).
8. Tang, G. H., Li, X. F., He, Y. L. and Tao, W. Q., "Electroosmotic Flow of Non-Newtonian Fluid in Microchannels," *Journal Non-Newtonian Fluid Mechanics*, **157**, pp. 133–137 (2009).
9. Park, H. M. and Lee, W. M., "Helmholtz-Smoluchowski Velocity for Viscoelastic Electroosmotic Flows," *Journal of Colloid and Interface Science*, **317**, pp. 631–636 (2008).
10. Park, H. M. and Lee, W. M., "Effect of Viscoelasticity on the Flow Pattern and the Volumetric Flow Rate in Electroosmotic Flows Through a Microchannel," *Lab on a Chip*, **8**, pp. 1163–1170 (2008).
11. Liu, Q. S., Jian, Y. J. and Yang, L. G., "Time Periodic Electroosmotic Flow of the Generalized Maxwell Fluids Between Two Micro-Parallel Plates." *Journal Non-Newtonian Fluid Mechanics*, **166**, pp. 478–486 (2011).
12. Jian, Y. J., Liu, Q. S. and Yang, L. G., "AC Electroosmotic Flow of Generalized Maxwell Fluids in a Rectangular Microchannel," *Journal Non-Newtonian Fluid Mechanics*, **166**, pp. 1304–1314 (2011).
13. Afonso, A. M., Alves, M. A. and Pinho, F. T., "Analytical Solution of Mixed Electroosmotic Pressure Driven Flows of Viscoelastic Fluids in Microchannels," *Journal of Colloid and Interface Science*, **159**, pp. 50–63 (2009).
14. Bird, R. B., Dotson, P. J. and Jonson, N. L., "Polymer Solution Rheology Based on a Finitely Extensible Bead-Spring Chain Model," *Journal Non-Newtonian Fluid Mechanics*, **7**, pp. 213–235 (1980).
15. Dhinakaran, S., Afonso, A. M., Alves, M. A. and Pinho, F. T., "Steady Viscoelastic Fluid Flow Between Parallel Plates Under Electroosmotic Forces: Phan-Thien-Tanner Model," *Journal of Colloid and Interface Science*, **344**, pp. 513–520 (2010).
16. Olivares, M. L., Vera-Candioti, L. and Berli, C. L. A., "The EOF of Polymer Solutions," *Electrophoresis*, **30**, pp. 921–929 (2009).
17. Sousa, J. J., Afonso, A. M. and Pinho, F. T., "Effect of the Skimming Layer on Electro-Osmotic-Poiseuille Flows of Viscoelastic Fluids," *Microfluidics and Nanofluidics*, **10**, pp. 107–122 (2011).
18. Liu, Q. S., Jian, Y. J. and Yang, L. G., "Alternating Current Electroosmotic Flow of the Jeffreys Fluids Time Through a Slit Microchannel," *Physics of Fluids*, **23**, 102001 (2011).
19. Akbar, N. S. and Nadeem, S., "Jeffrey Fluid Model for Blood Flow Through a Tapered Artery with a Stenosis," *Journal of Mechanics in Medicine and Biology*, **11**, pp. 529–545 (2011).
20. Berli, C. L. A. and Olivares, M. L., "Electrokinetic Flow of Non-Newtonian Fluids on Microchannels," *Journal of Colloid and Interface Science*, **320**, pp. 582–589 (2008).
21. Jian, Y. J., Yang, L. G. and Liu, Q. S., "Time Periodic Electroosmotic Flow Through a Microannulus," *Phyics of Fluids*, **22**, 042001 (2010).
22. Bird, R. B., Armstrong, R. C. and Hassager, O., *Dynamics of Polymeric Liquids. Volume 1: Fluid Mechanics*, 2nd Edition, John Wiley & Sons, Inc., New York (1987).
23. Bird, R. B., Stewart, W. E. and Lightfoot, E. N., *Transport Phenomena*, 2nd Edition, John Wiley & Sons, Inc., New York (2011).

(Manuscript received March 28, 2012,
accepted for publication July 23, 2012.)

https://doi.org/10.1017/jmech.2012.138 Published online by Cambridge University Press